

Scientific Report

Concerning the implementation of the project: January – December 2013

Two electrochemical methods were used for obtaining cobalt oxide-platinum composites on boron-doped diamond polycrystalline films, in order to assess the influence of the obtaining conditions on their specific properties. The first method, previously described in detail consisted in the potentiostatic deposition of Co_3O_4 (applied potential, 1.45 V) from a 0.25 M NaHCO_3 + 2 mM $\text{Co}(\text{NO}_3)_2$ solution, followed by platinum deposition, from a 1 M NaOH + 4.8 mM H_2PtCl_6 solution, at an applied potential of -0.7 V. Oxide and platinum loadings were controlled by adjusting the deposition time, and the electrodes thus obtained will be further referred as $\text{Pt}/\text{Co}_3\text{O}_4/\text{BDD}$. The same method was employed for platinum deposition on bare BDD and these electrodes (Pt/BDD) were also used in some experiments, for comparison. Chronoamperometric curves were recorded and the platinum loading was calculated from the deposition charge, estimated as the difference between the cathodic charge in the presence of $\text{Pt}(\text{IV})$ and that in its absence.

The second method consisted in performing several consecutive cyclic voltammetric runs (10 to 25, in a typical experiment), at a sweep rate of 50 mV s^{-1} , in an aqueous 0.25 M NaHCO_3 solution, containing 2 mM $\text{Co}(\text{NO}_3)_2$ and H_2PtCl_6 . The potential sweeps were

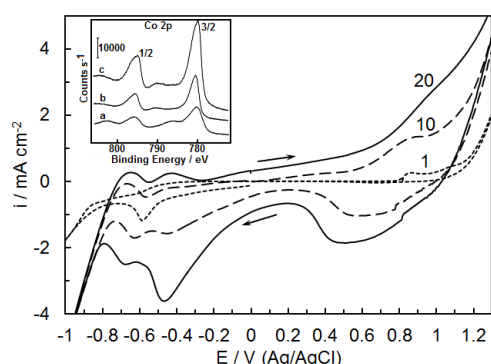


Fig. 1 Voltammograms recorded in 1 M NaOH +2 mM $\text{Co}(\text{NO}_3)_2$ +3.2 mM H_2PtCl_6 during 1st, 10th and 20th $\text{Pt}-\text{Co}_3\text{O}_4$ composite deposition cycles. (Inset: Co 2p XPS spectra for potentiodynamically (a), potentiostatically (b) and thermally (c) obtained Co_3O_4).

initiated from 0.0 V, the anodic and cathodic limits being 1.5 V and -1.0 V, respectively. The ratio of deposited cobalt oxide to deposited platinum was controlled by appropriately adjusting the concentration of platinum precursor from the deposition bath, and the electrodes thus obtained are referred as $\text{Pt}-\text{Co}_3\text{O}_4/\text{BDD}$. The platinum loading was again calculated from the deposition charge, estimated by comparing the cyclic voltammograms recorded during composite formation with those obtained (under the same experimental conditions) in the absence of $\text{Pt}(\text{IV})$ species.

As Fig. 1 illustrates, consecutive voltammetric runs performed in a 1 M NaOH solution in the presence of $\text{Co}(\text{NO}_3)_2$ and H_2PtCl_6 led to progressive deposition of both cobalt oxide and platinum. This process is clearly evidenced by the gradual enhancement of the cathodic peaks located at potential values higher and lower than *ca.* -0.05 V, which are characteristic of the presence of deposited Co_3O_4 and Pt, respectively. It was also observed that by continuous cycling the

capacitive-like background current (within the potential range *ca.* 0.1 to *ca.* 0.3 V) also increases, due to the corresponding increase of the composite film thickness. A reasonable explanation for this behavior is provided by the observation that, for electrochemically obtained cobalt oxide films, the mechanism of charge storage involves bulk intercalation of protons into the solid phase. Being more or less amorphous, anodically deposited Co_3O_4 has a rather loose structure and this is why, increasing loading will also result in an increased thickness of the oxide layer accessible to protons and, consequently, in an enhanced capacitive current. After 20 deposition cycles, the deposited film was investigated by XPS and a typical result in the Co 2p region is shown in the inset in Fig. 1 (curve a), together with the spectra recorded for Co_3O_4 films prepared by potentiostatic or thermal methods (curves b and c, respectively). The clear resemblance between the narrow-scan spectra demonstrates Co_3O_4 electrochemical formation.

Due to the particular obtaining conditions, both the potentiostatic and the potentiodynamic procedure will result in the deposition of hydrous cobalt oxide and, rigorous assessment of the loading would require heating or annealing. Nevertheless, since our interest was directed towards anodically formed hydrated cobalt oxide films we have avoided thermal treatments and the surface coverage of cobalt sites (Γ_{Co}) was used as a measure of the amount of deposited Co_3O_4 . Γ_{Co} was calculated from the charge under the

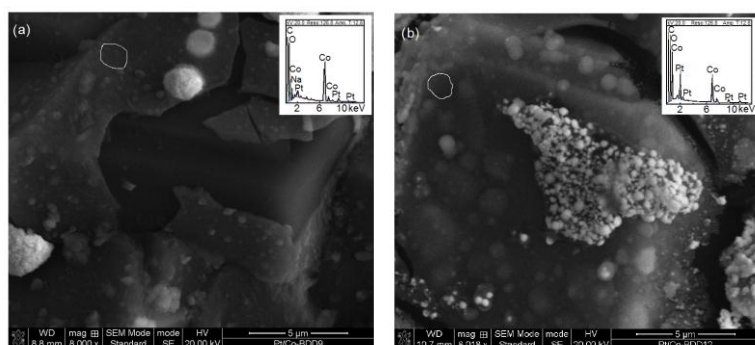


Fig. 2 Characteristic SEM micrographs for Pt/ Co_3O_4 /BDD (a) and Pt- Co_3O_4 /BDD (b) electrodes obtained after stabilization of the voltammetric response. Surface concentration of cobalt sites (nmol cm^{-2}): a) 29.2 and b) 29.4. Platinum loading ($\mu\text{g cm}^{-2}$): a) 28.3 and b) 27.8. Insets: EDS spectra recorded for areas bounded by the white contour lines.

peak corresponding to the $\text{Co}_3\text{O}_4/\text{CoOOH}$ transition (labeled A in Fig. 4) exhibited by cyclic voltammograms in alkaline media, keeping in mind that only one out of three Co sites is undergoing oxidation. Platinum loading was gauged based on the corresponding value of the deposition charge. We should note, however, that due to the inability to accurately evaluate the amount of charge that might be used for the underpotential deposition of

hydrogen, a certain degree of interference from this process cannot be completely ruled out. This is why, the proportion of cobalt to platinum was also determined from XPS measurements and only electrodes (Pt/ Co_3O_4 /BDD and Pt- Co_3O_4 /BDD) with similar Co to Pt ratios were further compared on a relative basis.

Fig. 2 shows typical SEM images obtained after the stabilization of the voltammetric response for Pt/ Co_3O_4 /BDD (Fig. 2a) and Pt- Co_3O_4 /BDD (Fig. 2b) electrodes with similar surface concentration of cobalt sites (29.2 and 29.4 nmol cm^{-2} , respectively) and comparable platinum loadings (28.3 and 27.8 $\mu\text{g cm}^{-2}$, respectively). It can be observed that in both

cases the BDD surface is covered by a more or less continuous oxide layer of rather uniform thickness, although some cracks are also evident on the micrographs, mainly on the edges and at the boundaries of the diamond crystallites. However, in the context of the present work this is not a matter of concern because the surface area of bare diamond exposed to the solution is very small and, due to specific features of BDD, its contribution to the overall electrochemical response is negligible. It also appears, that potentiostatic deposition of platinum on a previously deposited Co_3O_4 film results in large particles and favors the formation of Pt clusters (Fig. 2a). On the contrary, as Fig. 2b illustrates, cyclic voltammetry enabled the deposition of significantly smaller, and more uniform in size, Pt particles.

To better characterize the composites, EDS analysis was also performed, and insets in Fig. 2 show characteristic spectra recorded for areas of the coatings in which no Pt particles are observable on the SEM micrographs. It is worthy of note that, within these zones, the ratio between Co and Pt atomic percentages was typically found to be of *ca.* 6.6 to 0.3 and *ca.* 5.2 to 1.2 for Pt/ Co_3O_4 /BDD and Pt- Co_3O_4 /BDD, respectively. This indicates that, in the latter case, there is a higher amount of platinum nanoparticles embedded in the cobalt oxide film. This was not surprising because, due to the particular cyclic voltammetric conditions, the overall process of composite electroformation consisted in several sequences of alternating depositions of Co_3O_4 and Pt.

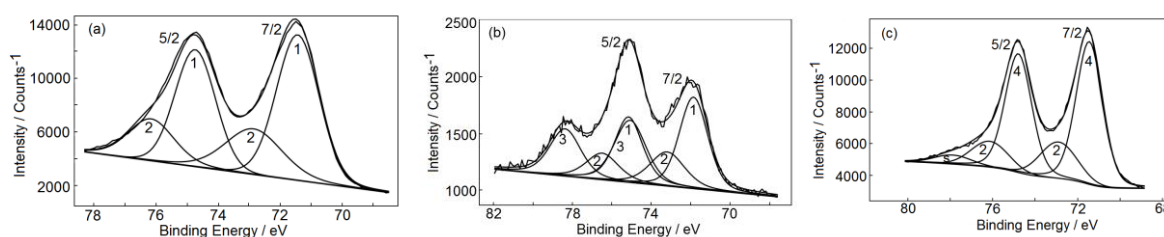


Fig. 3 Narrow-scan XPS spectra in the Pt 4f region for Pt/BDD (a), Pt/ Co_3O_4 /BDD (b) and Pt- Co_3O_4 /BDD (c) electrodes. The spectra were fitted by overlapping Gaussian-Lorentzian curves assigned to: (1) metallic Pt clusters, (2) $\text{Pt}(\text{OH})_2$, (3) PtO_2 and (4) Pt suboxides. Platinum loading ($\mu\text{g cm}^{-2}$): a) 27.6, b) 28.3 and c) 27.8. Surface concentration of cobalt sites (nmol cm^{-2}): b) 29.2 and c) 29.4

The effect of the deposition conditions on the composition of the coatings was also investigated, and XPS was employed in order to analyze platinum chemical states and their relative surface concentration for both composites. For better comparison, Fig. 3 shows a typical narrow-scan spectrum in the Pt 4f region recorded for platinum particles electrochemically deposited on bare BDD (Fig. 3a), together with those obtained for Pt/ Co_3O_4 /BDD and Pt- Co_3O_4 /BDD (Figs. 3b and 3c, respectively). As Fig. 3a illustrates, for Pt/BDD the spectrum could be deconvoluted into only two doublets, as previously reported for Pt particles deposited on conductive diamond by cyclic voltammetry. The most intense (at 71.3 and 74.7 eV) is characteristic to metallic platinum clusters, whereas the second one (with BE 72.9 and 76.3 eV) corresponds to Pt(II) oxidation state which is most likely present as $\text{Pt}(\text{OH})_2$. It therefore appears that, in the absence of the cobalt oxide substrate, elemental platinum prevails in terms of relative surface concentration (69.2%) and oxidized Pt is

present only as Pt(OH)₂ (30.8%). For Pt/Co₃O₄/BDD (Fig. 3b), a lower content of metallic platinum was found (45.1%) and, besides Pt(OH)₂ (21.0%), Pt(IV) oxidation state was also evidenced, the additional doublet from the spectrum (with BE 75.1 and 78.3 eV) being ascribed to the presence of PtO₂, with a relative surface concentration of 33.9%. It is interesting to note that for Pt–Co₃O₄ composites obtained by cyclic voltammetry (in which case, during each cycle both cobalt oxide and platinum were deposited) the surface concentration of Pt(OH)₂ species was of *ca.* 24.1%, and no elemental Pt was observed on the surface (Fig. 3c). Concerning the most intense doublet (labeled 4 in Fig. 3c), the assignment of the binding energy for the Pt 4f_{7/2} line (BE, 71.5 eV), as well as the ratio O/Pt after quantification, revealed the presence on a non-stoichiometric oxide (relative concentration, *ca.* 75.9%) formally referred as Pt suboxide. This was not unexpected because, due to the particular obtaining conditions, every stage of the Pt deposition process was followed by a strong anodic polarization (up to 1.5 V) necessary for the Co₃O₄ deposition to occur. Moreover, the cathodic limit of the voltammetric scans (-1.0 V) was not low enough to ensure efficient full reduction of the oxidized species of platinum.

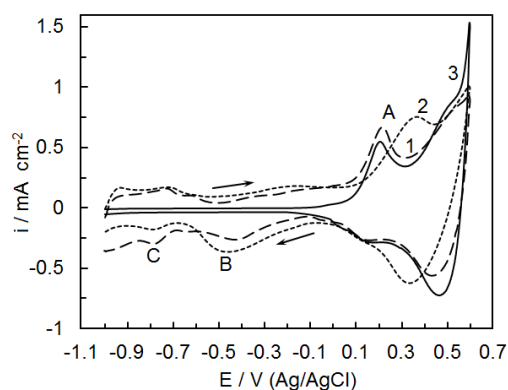


Fig. 4 Cyclic voltammograms recorded in 1 M NaOH (sweep rate, 50 mV s⁻¹) for Pt/Co₃O₄/BDD (1), Pt–Co₃O₄/BDD (2) and Co₃O₄/BDD (3) electrodes. Surface concentration of cobalt sites (nmol cm⁻²): 1) 26.5, 2) 26.7 and 3) 26.0. Platinum loading (μg cm⁻²): 1) 25.8 and 2) 25.3

The influence of the obtaining conditions on the overall electrochemical behavior of the composites was firstly checked by cyclic voltammetry in 1 M NaOH solution, at a sweep rate of 50 mV s⁻¹, within the potential range from -1.0 to 0.6 V. Fig. 4 shows characteristic voltammetric patterns recorded for Pt/Co₃O₄/BDD (curve 1) and Pt–Co₃O₄/BDD (curve 2) with similar oxide loadings (26.5 and 26.7 nmol cm⁻², respectively) and comparable platinum loadings (25.8 and 25.3 μg cm⁻², respectively). A typical voltammogram recorded for a Co₃O₄-modified BDD electrode (*I*_{Co}⁻, 26.0 nmol cm⁻²) under the same experimental conditions is also shown, for comparison (curve 3). It

appears that, at potential values higher than *ca.* -0.05 V, the shape of the voltammetric responses from Fig. 4 is quite similar to that usually observed for Co₃O₄ deposited (by thermal or electrochemical methods) on various substrates. This feature enabled us to estimate the cobalt oxide loading, based upon the voltammetric charge (corrected for the capacitive-like background current) corresponding to the anodic peak labeled A (see above). Conversely, at potential values lower than *ca.* -0.05 V, the voltammetric behavior of both composites is obviously dictated by the presence of platinum, which results in the occurrence of two characteristic cathodic peaks (labeled B and C) generally ascribed to platinum oxides reduction and to hydrogen adsorption on the oxide-free Pt surface, respectively.

Based upon the reversible charge integrated from voltammograms in Fig. 4 (as the average of the anodic and cathodic charges within the potential range -1.0 to 0.55 V), specific capacitances of 4.8 and 5.2 mF cm⁻² were estimated for Pt/Co₃O₄/BDD and Pt-Co₃O₄/BDD, respectively. There are reasons to believe that this behavior can be accounted both to the better dispersion of the Pt particles and to the fact that the bulk of the oxide is more accessible to proton diffusion when Co₃O₄ is potentiodynamically deposited. Although specific capacitances are well below those required for electrochemical capacitors applications, the slight, but nonetheless significant improvement of *ca.* 8% is encouraging because it proves that appropriate adjustment of the deposition conditions could enable more efficient use of the electrochemically active material.

Boron-doped diamond polycrystalline films were also used as support for TiO₂-Pt composites electrodeposition by a straightforward method previously described in detail.

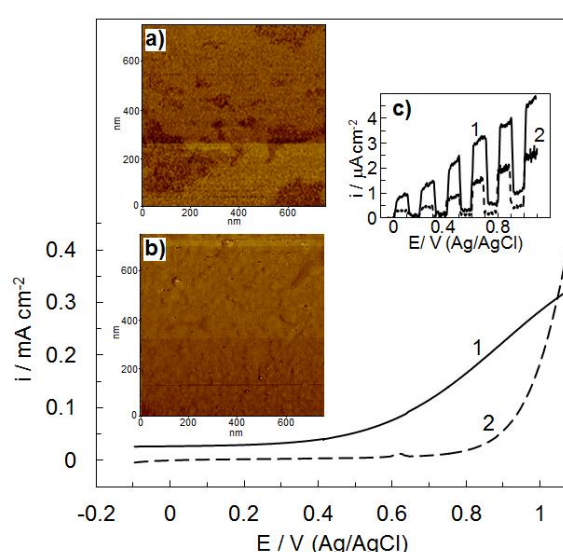


Fig. 5 Linear sweep voltammograms recorded at BDD electrodes in a 0.1 M KCl + 50 mM TiCl₃ solution (pH 2.2) in the presence (1) and in the absence (2) of SDS (sweep rate, 10 mV s⁻¹). Insets a and b: AFM amplitude images of TiO₂:SDS/BDD (a) and TiO₂/BDD (b) electrodes. Inset c: current-potential dependence upon intermittent illumination for TiO₂:SDS/BDD (1) and TiO₂/BDD (2) recorded in 0.1 M KCl at a sweep rate of 10 mV s⁻¹.

It appears that, during its initial stage, Ti(III) anodic oxidation is thermodynamically favored by the anionic surfactant, as indicated by the corresponding shift towards lower values of the onset potential. Nevertheless, the sigmoid shape of the linear sweep voltammogram (curve 1 in Fig. 5) clearly suggests that, in the presence of SDS, the overall process of titanium oxide formation is much slower and tends to become diffusion-controlled even at potential values close to *ca.* 1.0 V, which is obviously not the case when Ti(III) oxidation is carried out in the absence of the surfactant (compare curves 1 and 2 from Fig. 5).

Briefly, a TiO₂ amorphous film was anodically deposited (applied potential, 0.9 V) from a 0.1 M KCl + 50 mM TiCl₃ solution (pH, 2.2), both in the absence and in the presence (0.25 mM) of sodium dodecyl sulfate (SDS) and the amount of deposited oxide was controlled by appropriately adjusting the deposition time. Electrodes thus obtained will be further denoted as TiO₂/BDD and TiO₂:SDS/BDD, respectively. Platinum deposition was then carried out potentiostatically from a 0.1 M KCl + 4.8 mM H₂PtCl₆ solution, at an applied potential of -0.5 V.

The role that sodium dodecyl sulfate plays in the anodic oxidation of Ti(III) species was firstly checked by linear sweep voltammetry under quasi steady-state conditions (sweep rate, 10 mV s⁻¹) and Fig. 5 shows typical responses obtained both in the presence (curve 1) and in the absence (curve 2) of SDS.

Statistical analysis of the AFM results yielded root mean square roughness values of *ca.* 216 nm and 157 nm for TiO₂:SDS/BDD and TiO₂/BDD, respectively, in good agreement with the observation that surfactant-assisted oxide deposition enables higher porosity and, consequently, enhanced active surface area of the coating. More interesting is the fact that the results of the AFM measurements put into evidence incipient self-organization of the titanium oxide layer deposited in the presence of SDS. The photoelectrochemical activity of the BDD-supported titanium oxide coatings was examined in 0.1 M KCl under potentiodynamic regime (sweep rate, 10 mV s⁻¹) with intermittent UV irradiation, and typical responses recorded within the potential range -0.1 to 1.1 V are shown in inset c from Fig. 5. A significant enhancement of the photocurrent was observed for TiO₂:SDS/BDD electrodes (curve 1 from inset c), more important than would be expected from the increase of the roughness evidenced by AFM measurements. This behavior indicates that the higher photocurrent is due not only to the increased active surface area of the coating, but also to some improvement of the efficiency of charge carrier separation induced by the more organized structure of the TiO₂:SDS film.

Both types of titanium oxide were used as substrate for subsequent platinum potentiostatic deposition and, prior to further experiments, the electrodes thus obtained

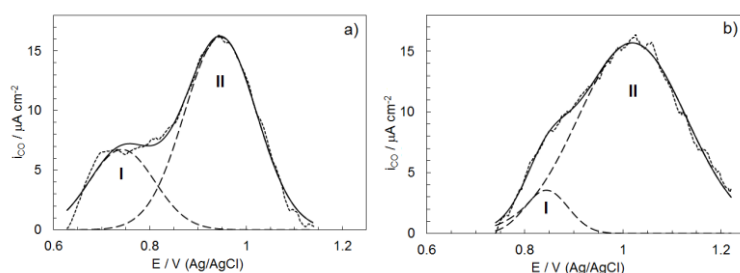


Fig. 6 Stripping voltammograms of adsorbed CO recorded in 0.5 M H₂SO₄ at a sweep rate of 20 mV s⁻¹ (dotted lines) at Pt/TiO₂:SDS/BDD (a) and Pt/TiO₂/BDD (b) electrodes. Platinum loading (µg cm⁻²): a) 16.25; b) 16.30. Solid lines represent voltammograms fitted by assuming two overlapping peaks (dashed lines).

(denoted as Pt/TiO₂:SDS/BDD and Pt/TiO₂/BDD) were stabilized by continuous cycling. To appraise the extent to which the electrocatalytic activity of Pt particles is affected by the deposition conditions of the titanium oxide substrate, anodic oxidation of adsorbed carbon monoxide, a process of paramount importance for direct methanol fuel cell

applications, was chosen as test-reaction. Stripping experiments were performed both with Pt/TiO₂:SDS/BDD and Pt/TiO₂/BDD electrodes and, to put the results into perspective, the current corresponding to CO oxidation (*i*_{CO}) was estimated as the difference between the voltammetric current obtained in the presence of the adsorbed CO and that recorded prior to its accumulation. For better comparison, the current was normalized to the active surface area of the platinum deposit estimated from the voltammetric charge associated to hydrogen desorption (see above) and typical results are shown in Fig. 6. It can be observed that, at both types of electrodes, CO oxidation give rise to rather broad peaks (dotted lines from Fig. 6), although TiO₂:SDS-supported platinum exhibits somewhat higher electrocatalytic activity, as indicated by the cathodic shift of the onset potential from *ca.* 0.74 V (for Pt/TiO₂/BDD) to *ca.* 0.63 V (for Pt/TiO₂:SDS/BDD).

The results of the stripping experiments were fitted by assuming two overlapping peaks (labeled I and II in Fig.6), corresponding to the oxidative desorption of weakly and strongly adsorbed CO species. An excellent agreement between experimental and calculated data was observed (compare dotted and continuous curves from Fig. 6), both for Pt/TiO₂:SDS/BDD ($R^2 = 0.9893$) and Pt/TiO₂/BDD ($R^2 = 0.9935$), and the peak potentials were found to be 0.74 and 0.84 V for peaks I, and 0.96 and 1.02 V for peaks II, respectively. It appears that, by switching from TiO₂ to TiO₂:SDS substrate, peaks I and II are significantly shifted towards lower potentials (with *ca.* 100 and *ca.* 60 mV, respectively) indicating a certain weakening of Pt–CO bonds. It is also interesting to note that at Pt/TiO₂:SDS/BDD electrodes *ca.* 26.55 % of the total stripping charge is associated to CO oxidation within the range of peak I, whereas, at Pt/TiO₂/BDD only *ca.* 8.53 % of the charge corresponds to the oxidation of weakly adsorbed CO. This is further proof that the use of surfactant-assisted electrodeposited TiO₂ substrate enhances the electrocatalytic activity for carbon monoxide oxidation of Pt particles and may perhaps ensure higher resistance to deactivation via CO poisoning during methanol oxidation. It seems reasonable to assume that this behavior is also due, at least in part, to the fact that Pt particles entrapped into the porous TiO₂:SDS matrix are more tightly surrounded by –OH groups. These groups could act as oxygen donors and may assist in the oxidative desorption of the CO, partially regenerating active sites from the electrocatalyst particle surface.

The results obtained in this stage of the research were published in the following papers:

- T. Spataru, M. Marcu, N. Spataru – "Electrocatalytic and photocatalytic activity of Pt–TiO₂ films on boron-doped diamond substrate" – *Applied Surface Science* **269** (2013) 171
- T. Spataru, M. Anastasescu, N. Spataru, A. Fujishima – "Influence of cobalt oxide substrate on the resistance to fouling during methanol oxidation of platinum particles" – *Electrochemistry Communications* **29** (2013) 1.
- T. Spătaru, L. Preda, P. Osiceanu, C. Munteanu, M. Anastasescu, M. Marcu, N. Spătaru – "Role of surfactant-mediated electrodeposited titanium oxide substrate in improving electrocatalytic features of supported platinum particles" – *Applied Surface Science*, <http://dx.doi.org/10.1016/j.apsusc.2013.10.092>